引用格式：LIN Yi, WANG Yiqun, MA Huilian. Back-reflection Noise Analysis of the Resonant Micro-optical Gyroscope with Different Modulation Techniques[J]. Acta Photonica Sinica, 2022, 51(9):0906004
林伊,汪逸群,马慧莲.谐振式微光学陀螺不同调制方式下背向反射噪声分析[J].光子学报,2022,51(9):0906004

谐振式微光学陀螺不同调制方式下背向反射噪声分析

林伊[1],汪逸群[1],马慧莲[2]
(1之江实验室 智能装备研究院,杭州 310000)
(2浙江大学 航空航天学院,杭州 310000)

摘　要:建立了基于反射式光波导环形谐振腔的谐振式微光学陀螺背向反射噪声分析模型,仿真分析了背向反射噪声强度项和干涉项在系统互易和非互易时的影响。比较了不同调制方式下,谐振式微光学陀螺系统中背向反射噪声的抑制情况,研究表明,分频调制下载波抑制的方式可将背向反射噪声抑制到极限灵敏度以下,同频调制下背向反射噪声受限于光开关/脉冲调制器的信道串扰。分别搭建了分频调制和同频调制系统,实验测试结果表明分频调制下陀螺输出稳定,同频调制下由于未对背向反射噪声强度项进行抑制,引入了10°/s量级的噪声,验证了理论仿真结果。

关键词:传感器;谐振式微光学陀螺;背向反射噪声;调制解调技术;时分复用技术
中图分类号:TN815　　**文献标识码**:A　　**doi**:10.3788/gzxb20225109.0906004

0 引言

谐振式微光学陀螺(Resonant Micro-optical Gyroscope,RMOG)作为光学陀螺的一种,相比于其他小型化陀螺所存在的问题,如激光陀螺由于模式竞争导致的闭锁效应[1],干涉式集成光学陀螺达到和RMOG相同精度所需的光波导长度[2-4],其在小型化和集成化上具有重要优势[5-7]。

RMOG采用了高相干光源,因此背向反射光与信号光之间会发生干涉,形成背向反射噪声[8-10]。目前RMOG系统仍采用混合集成方式,RMOG系统中的核心敏感器件光波导环形谐振腔(Waveguide Ring Resonator, WRR)通过光纤与其他器件相连接,背向反射噪声主要来自于芯片和光纤的耦合点处,若不加抑制措施,会引起百度每秒甚至上千度每秒的陀螺零偏变化。

为抑制背向反射噪声,除了提高工艺,降低波导损耗或端面斜抛以减小反射系数外,目前主要采用分频调制即顺逆时针采用不同的调制频率、载波抑制的方式[11-12]。但分频调制会破坏系统的互易性,采用同频调制即顺逆时针采用相同的调制频率可有效减小激光器频率噪声及相位调制器残余强度调制噪声[13]。本文建立了背向反射噪声的分析模型,分析了背向反射强度项和干涉项噪声的量级大小,比较了不同调制方式下背向反射噪声的抑制情况。研究表明,分频调制下载波抑制的方式可将背向反射噪声控制在极限灵敏度以下,同频调制下背向反射强度项会带来10°/s量级的噪声,且无法被抑制,采用光开关/脉冲信号发生器可同时抑制强度项和干涉项噪声,但目前其信道串扰较大,限制了其抑制效果。

1 基本原理

1.1 背向反射噪声模型

RMOG中背向反射噪声主要来自于WRR与光纤耦合点处的菲涅尔反射。图1为反射式WRR背向反

基金项目:之江实验室星间高速激光通信机项目(No.112004-AD2003),国家自然科学基金(No. 62175218)
第一作者:林伊(1994—),女,助理研究员,博士,主要研究方向为光纤传感技术。Email: linyi94@zju.edu.cn
收稿日期:2021-12-15;**录用日期**:2022-04-21

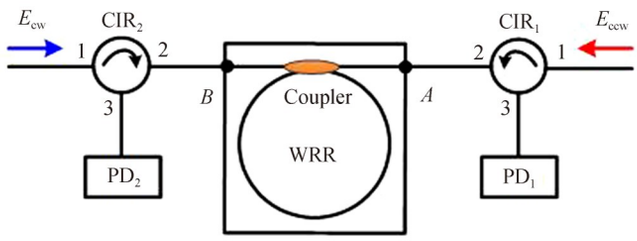

图1 反射式WRR背向反射噪声示意

Fig. 1 Back-reflection noise of reflection-type WRR

射噪声示意图。假设顺逆时针光路分光比分别为u_R、u_L，反射点A、B光程为z，两反射点反射系数分别为α_A、α_B，谐振腔长度为L，波导单位损耗为α_1，耦合器的耦合系数及损耗分别为k、α_C，顺逆时针输入光相位分别为θ_A、θ_B，相位差为$\Delta\theta$。只考虑一次反射，输入光电探测器PD$_1$的光场由顺时针方向入射光经环形器CIR$_1$端口3的输出光E_S，以及逆时针方向入射光的反射光场E_{BS}组成，其中E_{BS}包括逆时针方向入射光经A点的反射光E_A，以及逆时针方向入射光经B点的反射光再由A点的输出E_{ABA}，可分别表示为

$$E_S = u_R^{1/2} E_0 e^{j(\omega t+\theta_B)} \sqrt{1-\alpha_A}\sqrt{1-\alpha_B}\sqrt{1-\alpha_1 \cdot z}\, e^{-j2\pi\frac{z}{\lambda}} h(\Delta f) \tag{1}$$

$$\begin{aligned} E_{BS} &= E_A + E_{ABA} = -u_L^{1/2} E_0 e^{j(\omega t+\theta_A)}\sqrt{\alpha_A} + u_L^{1/2} E_0 e^{j(\omega t+\theta_A)}\sqrt{1-\alpha_A}(1-\alpha_1 \cdot z) h^2(\Delta f)\sqrt{\alpha_B}\, e^{j\left(-4\pi\frac{z}{\lambda}\right)}\sqrt{1-\alpha_A} \\ &= -u_L^{1/2} E_0 e^{j(\omega t+\theta_A)}\left(\sqrt{\alpha_A} - (1-\alpha_A)(1-\alpha_1 \cdot z)\sqrt{\alpha_B}\, h^2(\Delta f) e^{j\left(-4\pi\frac{z}{\lambda}\right)}\right) \end{aligned} \tag{2}$$

式中，$h(\Delta f)$为反射式WRR关于频率的传递函数，可表示为[14]

$$h(\Delta f) = T - R\frac{e^{-j2\pi\cdot\frac{\Delta f}{FSR}}}{1-Qe^{-j2\pi\cdot\frac{\Delta f}{FSR}}} \tag{3}$$

式中，

$$T = \sqrt{(1-k)(1-\alpha_C)} \tag{4}$$

$$R = k(1-\alpha_C)\sqrt{1-\alpha_1 L} \tag{5}$$

$$Q = \sqrt{(1-k)(1-\alpha_C)(1-\alpha_1 L)} \tag{6}$$

FSR为WRR的自由频谱范围，定义为相邻两谐振点间的频差。那么在PD$_1$测得的总光强为

$$I_{PD_1}(z,t) = c\varepsilon_0 |E_S + E_{BS}|^2 = c\varepsilon_0(E_S \cdot E_S^*) + c\varepsilon_0(E_S \cdot E_{BS}^* + E_{BS} \cdot E_S^*) + c\varepsilon_0(E_{BS} \cdot E_{BS}^*) = I_1 + I_2 + I_3 \tag{7}$$

式中，I_1为待测信号光强，I_2为信号光和背向反射光的相干光强，可简称为干涉项，I_3为背向反射光强，可简称为强度项。同理可得到在PD$_2$处测得的光强。

图2为RMOG的检测原理，图中黑色实线为理想情况下顺逆时针待检测信号I_1，红色和蓝色虚线为叠加了噪声后的顺逆时针路谐振曲线，顺逆时针的谐振谷位置相对于待测信号谐振谷的频率偏移可分别表示为

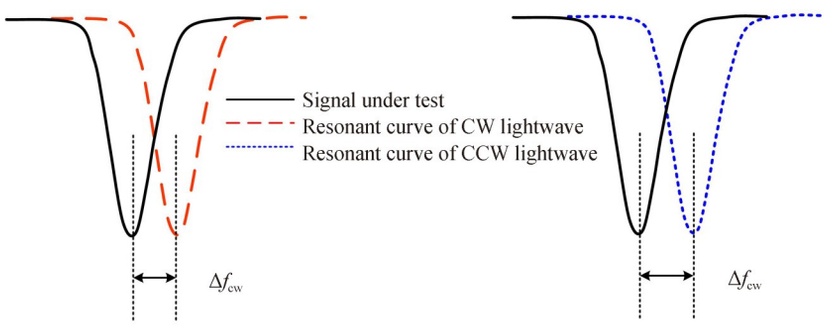

图2 RMOG检测原理

Fig. 2 Detection principle of the RMOG

Δf_{CW}和Δf_{CCW}，两者的差异最终等效为陀螺输出偏置误差，可表示为

$$\Omega=(\Delta f_{CW}-\Delta f_{CCW})/k_{SF} \tag{8}$$

式中，k_{SF}为陀螺标度因数。

1.2 背向反射噪声强度项

当系统互易时，即顺逆时针分光比一致，芯片与光纤的两个耦合点反射系数一致时，仿真了背向反射噪声强度项与谐振频率差之间的关系，结果如图3。由图3(a)、(b)可知，在两反射点光程$z=(n+m/4)\lambda$(n为任意整数，$m=0,1,2,3$)时，此时不论两路光传输相位差为何值，反射信号I_3关于谐振频率偏差为零的直线左右对称，即I_3不会对检测信号I_1产生非互易性影响；当两反射点光程z为其他值时，两路光传输相位为任意值，反射信号虽然不关于谐振频率偏差为零的直线左右对称，但对于顺逆时针的影响一致，如图3(c)所示，因此对检测顺逆时针光波的谐振点频率偏差获得陀螺的转动信息无影响。

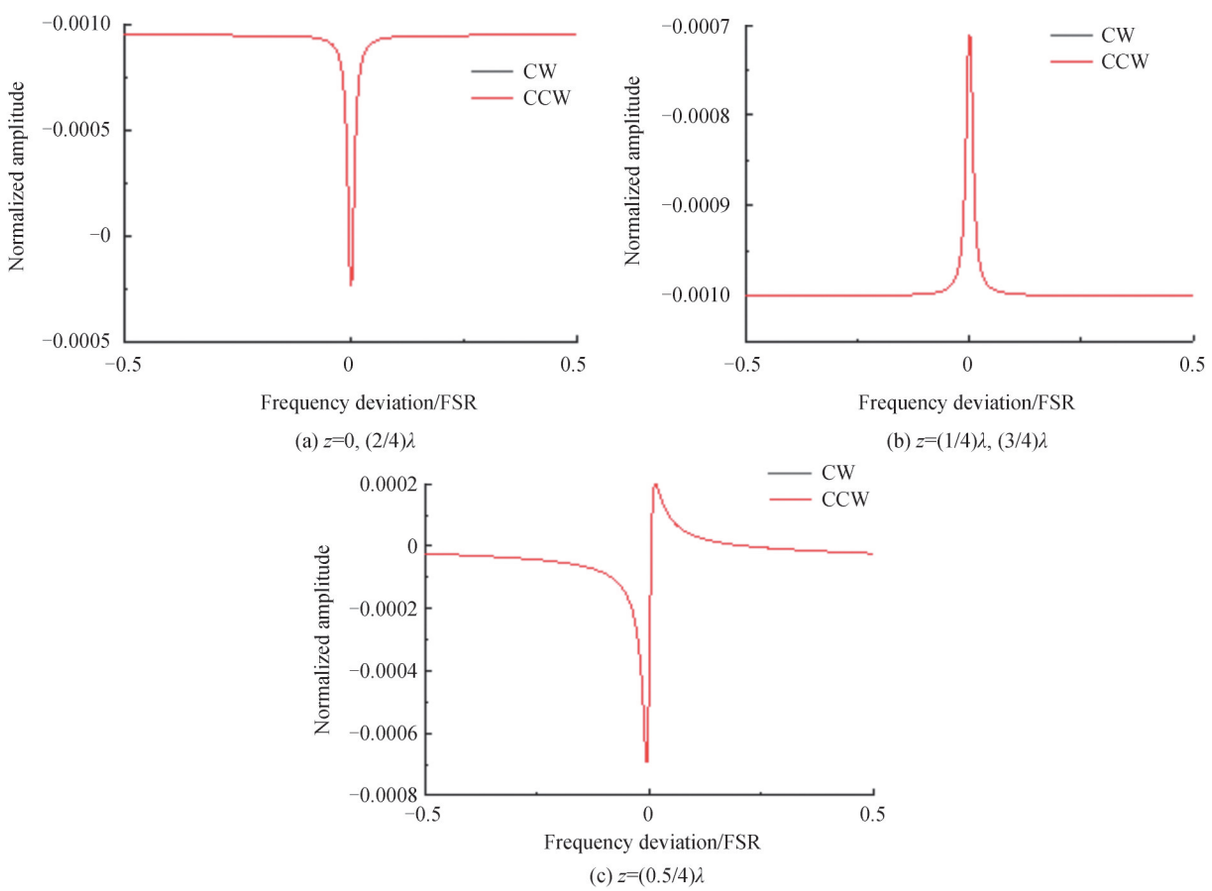

图3 I_3与谐振频率差之间的关系曲线

Fig. 3 Relationship between I_3 and the frequency deviation

当系统非互易时，根据实际系统测试顺逆时针分光比为2∶3，耦合器耦合系数为2%，耦合器损耗为0.1 dB，光波导损耗为0.01 dB/cm，假设背向反射系数为30 dB，以直径为5.06 cm的WRR芯片为例，其标度因数为392 Hz/(°)/s。图4为背向反射噪声强度项引起的陀螺输出偏置误差与两反射点间间距的关系曲线，与两路光传输相位差无关，图中已将频率偏移量转化为相应的角速度偏移量。可以看出，系统非互易时，背向反射强度项可引起10°/s量级的噪声。

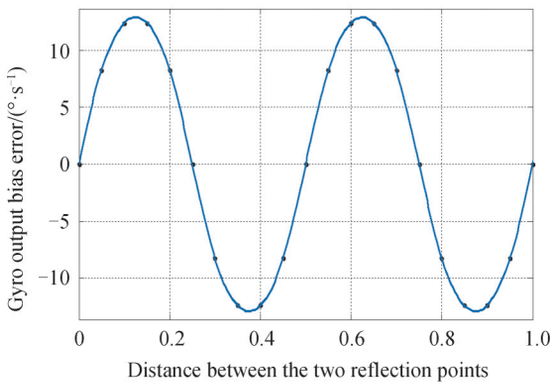

图4 背向反射噪声强度项引起的陀螺输出偏置误差与两反射点间间距的关系

Fig. 4 The relationship of the gyro output bias error induced by the intensity item of the back-reflection noise and the distance between the two reflection points

1.3 背向反射噪声干涉项

如图5所示，仿真了系统互易和非互易（顺逆时针分光比为2∶3）时，背向反射噪声干涉项引起的陀螺输出偏置误差和顺逆时针光传输相位差之间的关系曲线，可以看出，系统非互易相比系统互易时会引入更大的背向反射噪声。图中假设两反射点间距$z=n\lambda$，此时可引入最大的偏置误差峰峰值，系统互易和非互易时分别对应257 °/s、261 °/s的偏置误差峰峰值。

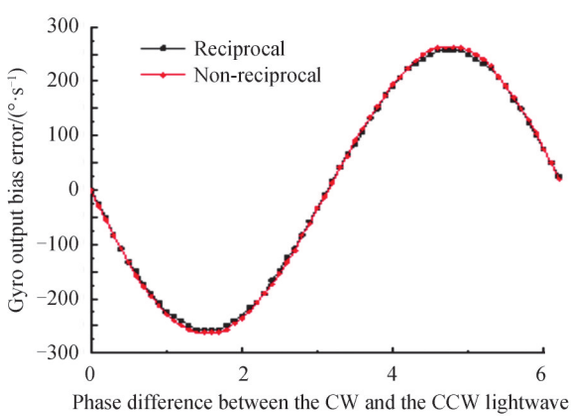

图5 背向反射噪声干涉项引起的陀螺输出偏置误差和顺逆时针光传输相位差之间的关系

Fig. 5 The relationship of the gyro output bias error induced by the interference item of the back-reflection noise and the phase difference between the CW and the CCW lightwave

2 不同调制方式比较

2.1 分频调制

由以上分析可知，背向反射噪声可分为强度项和干涉项两部分。为抑制强度项噪声，一般对顺逆时针采用不同频率的调制信号，此时可认为背向反射光本身对陀螺输出无影响；为抑制干涉项噪声，可以采取载波抑制的方式，抑制效果与载波抑制比有关，可表示为[15]

$$\mathrm{BIAS_{BS}}=\Omega_{\mathrm{BS}}\left(\frac{\Delta V}{V}\right)^{N} \tag{9}$$

式中，Ω_{BS}为未采取抑制措施时的背向反射噪声，当系统非互易时，由2.3节可知背向反射干涉项噪声引入的陀螺输出偏置误差峰峰值为261 °/s，N表示载波抑制个数（$N=0,1,2$），$\Delta V/V$表示载波抑制的误差。图6为基于分频调制技术的RMOG原理框图。采用的激光器为光纤激光器，工作波长为1 550 nm。相位调制器（Phase Modulator，PM）的半波电压为2.3 V。光电探测器的带宽和增益是可调节的。激光器输出光通过Y分支相位调制器（Y-PM）分为顺逆时针两束光，Y-PM用于信号调制，与单臂相位调制器PM1和PM2都可起到载波抑制的作用，一共可达到120～160 dB的载波抑制比。环形器$\mathrm{CIR_1}$和$\mathrm{CIR_2}$耦合光进出WRR，两个

光电探测器，PD_1和PD_2将光信号转换为电信号，锁相放大器（Lock-in Amplifier，LIA）和低通滤波器（Low Pass Filter，LPF）在FPGA内实现。PD_2的输出通过伺服回路反馈给激光器使得激光器锁定在顺时针路的谐振频率处，PD_1的输出通过LIA1和LPF后作为陀螺输出。根据式（9），图7仿真了载波抑制比与背向反射噪声的关系曲线。当采用此WRR作为RMOG的核心敏感元件，在1 mW的探测功率下，其极限灵敏度[16]为1.76 °/h，由图7可以看出，当采用分频调制技术且载波抑制比达到120 dB时，背向反射噪声的影响可控制在极限灵敏度以下。

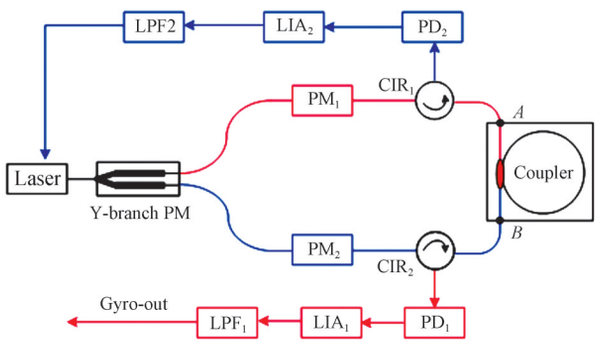

图6　基于分频调制技术的RMOG原理

Fig. 6　Schematic of the RMOG based on the separation modulation technique

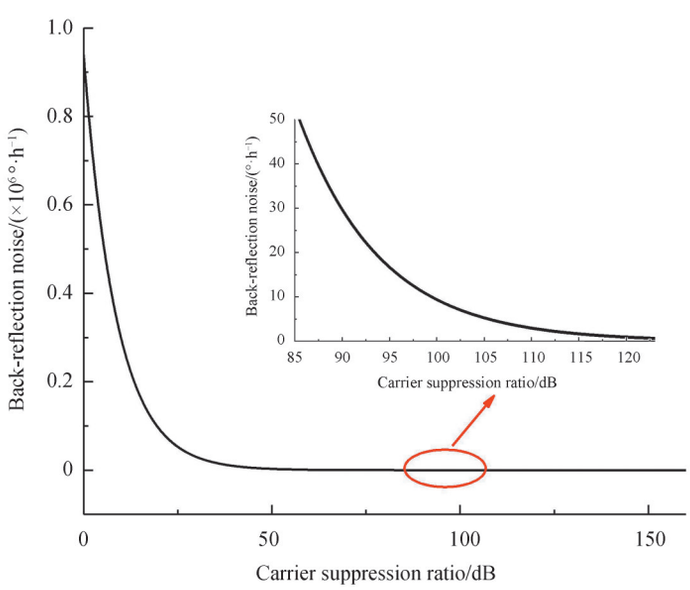

图7　背向反射噪声与载波抑制比的关系

Fig. 7　The relationship between the back-reflection noise and the carrier suppression ratio

2.2　同频调制

当采用同频调制，即顺逆时针光采用同一调制频率可提高系统互易性，能有效抑制相位调制器的残余强度调制噪声及激光器频率噪声。同频调制系统如图8，顺逆时针光在分光前先经过PM0同频调制，PM1和PM2上施加不同频率的调制信号进行载波抑制以抑制背向反射干涉项噪声，实际系统可通过额外增加单臂PM增大载波抑制比，但此系统对强度项噪声没有抑制效果。根据1.2节分析可知，当系统非互易时，背向反射强度项会带来10 °/s量级的噪声，因此有必要在同频调制系统中增加光开关[17]或脉冲光调制器对背向反射噪声强度项进行抑制。

图9为基于光开关/脉冲光探测的时分复用谐振式陀螺系统。通过光开关/脉冲光调制器可以使顺逆时针光束在时间上分开，避免信号光和背向反射光之间的能量耦合，相当于减小背向反射系数。理论上可完全抑制背向反射强度项及干涉项噪声，但受限于光开关/脉冲光调制器的信道串扰，顺逆时针光在时间切换时仍会有残余信号光，使得实际工作时谐振腔内并非只有理想的一个方向光波在传输，仍会引起背向反射

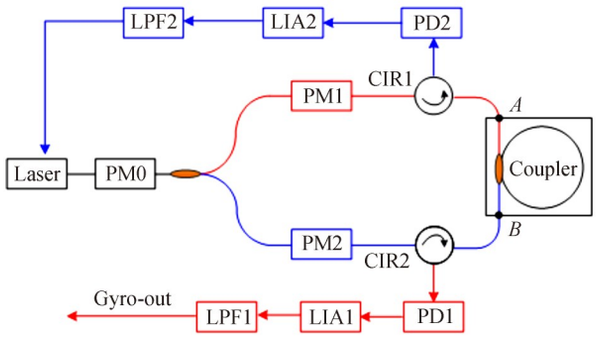

图 8 基于同频调制技术的RMOG原理

Fig. 8 Schematic of the RMOG based on the reciprocal modulation technique

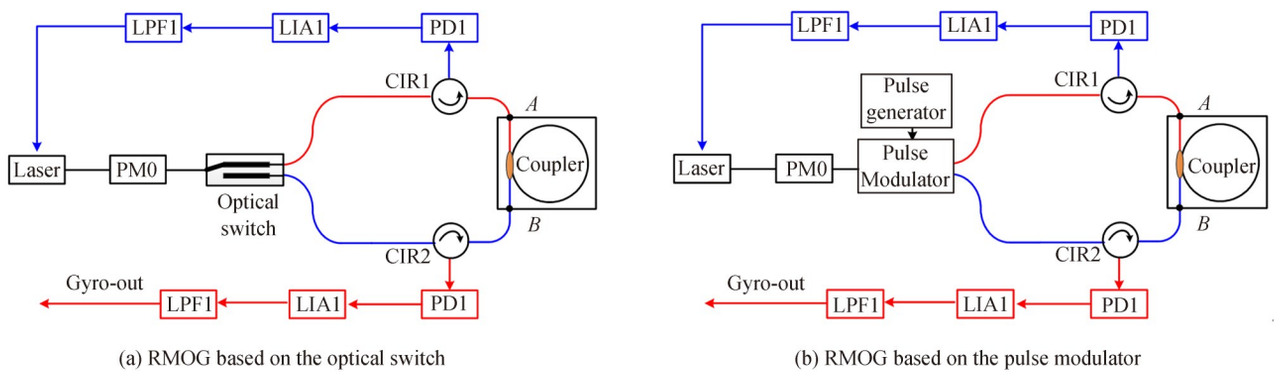

图 9 时分复用的RMOG系统

Fig. 9 Schematic of the time division multiplexing RMOG

噪声,因此式(7)可表示为

$$\begin{aligned} I_{\mathrm{PD_1}}(z,t) &= c\varepsilon_0\left|E_{\mathrm{S}}+E_{\mathrm{BS}}\right|^2 = c\varepsilon_0(E_{\mathrm{S}}\cdot E_{\mathrm{S}}^*)+c\varepsilon_0\sqrt{\alpha_{\mathrm{CT}}}\,(E_{\mathrm{S}}\cdot E_{\mathrm{BS}}^*+E_{\mathrm{BS}}\cdot E_{\mathrm{S}}^*)+c\varepsilon_0\alpha_{\mathrm{CT}}(E_{\mathrm{BS}}\cdot E_{\mathrm{BS}}^*) \\ &= I_1+I_2+I_3 \end{aligned} \tag{10}$$

式中,α_{CT}表示信道串扰。根据式(10)仿真了背向反射强度项和干涉项噪声与信道串扰的关系,结果如图10,可以看出当信道串扰达到45 dB时,背向反射噪声强度项即可降至极限灵敏度,而对于背向反射噪声干涉项则需要信道串扰优于115 dB才可将其影响降至极限灵敏度以下,因此对光开关/脉冲光调制器的指标提出

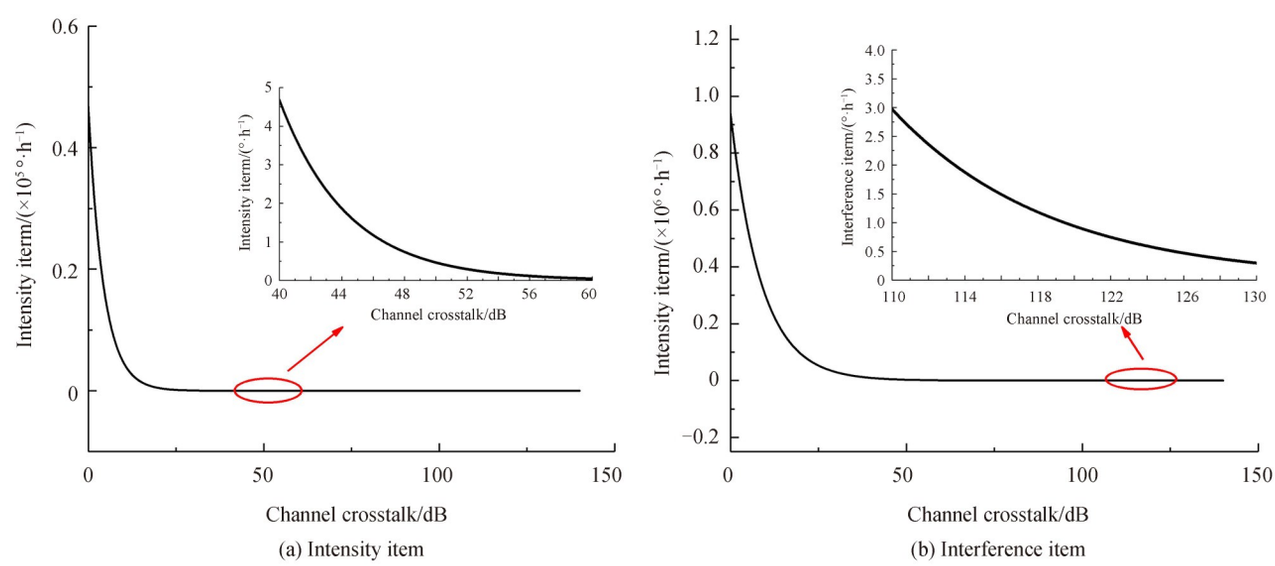

图 10 信道串扰与背向反射噪声的关系

Fig. 10 Relationship between the channel crosstalk and the back-reflection noise

了较为苛刻的要求。

3 实验测试

室温下分频调制和同频调制系统对应的系统框图如图6和图8。进行系统输出特性测试，测试时间为1 800 s，采样带宽为8 Hz，陀螺输出数据如图11示。可以看出，分频调制下，由于强度项和干涉项背向反射噪声得到有效抑制，陀螺输出稳定，同频调制下，由于没有对背向反射噪声强度项进行抑制，引入了10 °/s量级的噪声，和仿真结果吻合。由于目前商用光开关/脉冲光调制器的信道串扰很难满足同频调制系统的要求[17]，因此目前在谐振式微光学陀螺中分频调制方案仍占据主导优势。

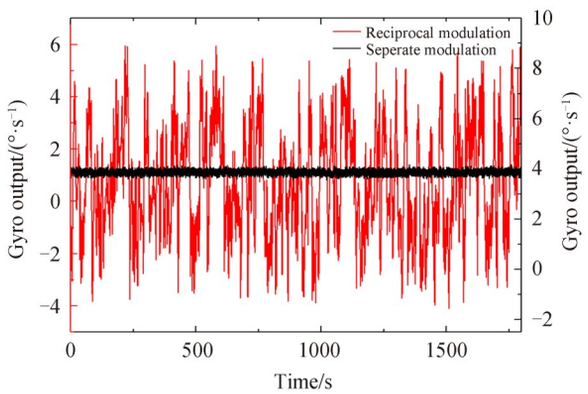

图11 分频调制和同频调制下陀螺输出测试

Fig. 11 Gyro out tests based the separate modulation and the reciprocal modulation techniques

4 结论

本文建立了RMOG中背向反射噪声模型，比较了分频调制和同频调制系统对背向反射噪声的抑制情况，为实际系统调制方式的选择提供了理论依据。分析表明，分频调制系统可将背向反射噪声影响控制到极限灵敏度以下，同频调制系统可提高系统互易性，但对背向反射噪声强度项无抑制作用，在同频调制系统中增加光开光/脉冲光调制器理论上可完全抑制背向反射噪声强度项和干涉项，但对光开光/脉冲光调制器的信道串扰指标提出了苛刻的要求。

参考文献

[1] CHOW W W, GEABANACLOCHE J, PEDROTTI M, et al. The ring laser gyro[J]. Reviews of Modern Physics, 1985, 57(1): 61-104.

[2] CIMINELLI C, DELL'OLIO F, CAMPANELLA C E, et al. Photonic technologies for angular velocity sensing[J]. Advances in Optics & Photonics, 2010, 2(2):370-404.

[3] MONOVOUKAS C, SWIECKI A K, MASEEH F. Integrated optical gyroscopes offering low cost, small size and vibration Immunity[C]. SPIE, 2000, 3936: 293-300.

[4] OHNO A, KUROKAWA A, KUMAGAI T, et al. Applications and technical progress of fiberoptic gyros in Japan[C]. 18th International Optical Fiber Sensors Conference, OSA Technical Digest, 2006.

[5] MA Huilian, ZHANG Jianjie, WANG Linglan, et al. Development and evaluation of optical passive resonant gyroscopes [J]. Journal of Lightwave Technology, 2017, 35(16): 3546-3554.

[6] ZHANG Jianjie, MA Huilian, LI Hanzhao, et al. Single polarization fiber-pigtailed high-finesse silica waveguide ring resonator for a resonant micro-optic gyroscope[J]. Optics Letters, 2017, 42(18): 3658-3661.

[7] CATERINA C, FRANCESCO P, ARMENISE M N. A new integrated optical angular velocity sensor[C]. SPIE, 2005, 5728: 93-100.

[8] TAKAHASHI M, TAI S, KYUMA K. Effect of Reflections on the drift characteristics of a fiber-optic passive ring-resonator gyroscope[J]. Journal of Lightwave Technology, 1990, 8(5):811-816.

[9] IWATSUKI K, HOTATE K, HIGASHIGUCHI M. Effect of Rayleigh backscattering in an optical passive ring-resonator gyro[J]. Applied Optics, 1984, 23(21): 3916-3924.

[10] ZHANG Xulin, ZHOU Kejiang. Analysis on two-reflection-dots model outside resonator of R-MOG[J]. Chinese Journal of Sensors and Actuators, 2009, 22(6): 811-815.

张旭琳,周柯江. 谐振式微光学陀螺环形谐振腔外双反射点模型分析[J]. 传感技术学报, 2009, 22(6): 811-815.
[11] MA Huilian, ZHANG Xulin, JIN Zhonghe, et al. Waveguide-type optical passive ring resonator gyro using phase modulation spectroscopy technique[J]. Optical Engineering, 2006, 45(8):1678-1678.
[12] MA Huilian, HE Zuyuan, HOTATE K. Reduction of backscattering induced noise by carrier suppression in waveguide-type optical ring resonator gyro[J]. Journal of Lightwave Technology, 2011, 29(1):85-90.
[13] LI Hanzhao, LIN Yi, LIU Lu, et al. Signal processing improvement of passive resonant fiber optic gyroscope using a reciprocal modulation-demodulation technique[J]. Optics Express, 2020, 28(12): 18103-18111.
[14] YARIV A. Critical coupling and its control in optical waveguide-ring resonator systems[J]. IEEE Photonics Technology Letters, 2002, 14(4): 483-485.
[15] KAISER T J, CARDARELLI D, WALSH J G. Experimental development in the RFOG[C]. SPIE, 1990, 1367: 121-126.
[16] XIE Chengfeng, TANG Jun, CUI Danfeng, et al. Resonant microsphere gyroscope based on a double faraday rotator system[J]. Optics Letters, 2016, 41(20): 4783-4786.
[17] QIAN Weiwen, WU Chuanbin, LIN Yi, et al. Resonant micro-optical gyroscope based on optical switch to suppress backscattering noise[J]. Chinese Journal of Lasers, 2020, 47(10): 1010003.
钱伟文,吴传斌,林伊. 基于光开关抑制背向散射噪声的谐振式微光学陀螺[J]. 中国激光,2020, 47(10): 1010003.

Back-reflection Noise Analysis of the Resonant Micro-optical Gyroscope with Different Modulation Techniques

LIN Yi[1], WANG Yiqun[1], MA Huilian[2]
(1 *Institute of Intelligent Equipment*, *Zhejiang Lab*, *Hangzhou* 310000, *China*)
(2 *School of Aeronautics and Astronautics*, *Zhejiang University*, *Hangzhou* 310000, *China*)

Abstract: The resonant micro-optical gyroscope has advantages in miniaturization and integration compared with other gyroscopes. The back-reflection noise is one of the main optical noises restricting the sensitivity of the resonant micro-optical gyroscope which mainly comes from the coupling points between the waveguide ring resonator and the tail fiber. The model of the back-reflection noise of the resonant micro-optical gyroscope based on the reflection-type waveguide ring resonator is established. The influences of the intensity item and the interference item of the back-reflection noise under the reciprocal system and the nonreciprocal system are analyzed, respectively. When the resonant micro-optical gyroscope system is reciprocal, the intensity item of the back-reflection noise has the same impact on the frequency deviation of the clockwise and the counter clockwise lightwave which counteracts, so it has no impact on measuring the rotation rate. When the system is nonreciprocal, the intensity item of the back-reflection noise introduces the noise of the magnitude of 10°/s. The interference item of the back-reflection noise introduces the noise of the magnitude of 257°/s and 261°/s respectively when the system is reciprocal and nonreciprocal. The suppression effects of the back-reflection noise in the resonant micro-optical gyroscope with different modulation techniques are compared. The separation modulation technique can suppress the intensity item of the back-reflection noise when using different modulation frequency and the interference item of the back-reflection noise can be suppressed below the shot-noise limited sensitivity when the carrier suppression reaches 120 dB which is achievable using four phase modulators. The reciprocal modulation technique can improve the reciprocity of the resonant micro-optical gyroscope and can suppress the residual intensity modulation noise of the phase modulator and the frequency noise of the laser effectively. When using the reciprocal modulation technique, the interference item of the back-reflection noise can be suppressed by carrier suppression but the intensity item of the back-reflection noise can not be suppressed which brings the noise of the magnitude of 10°/s according to the simulation result. So it is necessary to add the optical switch or the pulse modulator in the resonant micro-optical gyroscope system to suppress the intensity item when using the reciprocal modulation technique. The optical switch or the pulse modulator can separate the clockwise and the counter clockwise lightwave in time and avoid the energy coupling between the signal light and the back-reflection light which is equivalent to reducing the back-reflection coefficient. In theory, the intensity item and the interference item of the back-reflection

noise can be suppressed totally but the suppression effect is limited by the channel crosstalk of the optical switch or the pulse modulator. According to the simulation result, the intensity item of the back-reflection noise can be suppressed below the shot-noise limited sensitivity when the crosstalk of the optical switch or the pulse modulator is 45 dB. To suppress the interference item of the back-reflection noise below the shot-noise limited sensitivity the crosstalk of the optical switch or the pulse modulator should be better than 115 dB which is difficult to achieve. The above analyses provide the theoretical basis for the establishment of the resonant micro-optical gyroscope system. The resonant micro-optical gyroscopes using the separation modulation technique and the reciprocal modulation technique are established, respectively. The outputs of the two system are tested in 1 800 s. The test results show that the gyro output is stable under the separation modulation system because the intensity item and the interference item of the back-reflection noise are both suppressed. The noise of the magnitude of 10°/s is introduced in the system using the reciprocal modulation technique because the intensity item of the back-reflection noise is not suppressed which is coincident with the simulation result.

Key words: Sensor; Resonant micro-optical gyroscope; Back-reflection noise; Modulation and demodulation technique; Time division multiplexing technique

OCIS Codes: 060.2800; 060.5060; 130.4815; 230.5750; 280.1350

Foundation item: High-speed Satellite Laser Communication Terminal Program of Zhejiang Lab (No.112004-AD2003), National Natural Science Foundation of China (No. 62175218)